Applied Catalysis B: Environmental 97 (2010) 323–332

Contents lists available at ScienceDirect

Applied Catalysis B: Environmental

journal homepage: www.elsevier.com/locate/apcatb

Impact of CO on the transformation of a model FCC gasoline over $CoMoS/Al_2O_3$ catalysts: A combined kinetic and DFT approach

F. Pelardy[a], C. Dupont[b], C. Fontaine[a], E. Devers[b,*], A. Daudin[b], F. Bertoncini[b], P. Raybaud[b], S. Brunet[a,*]

[a] UMR CNRS 6503, Laboratoire de Catalyse en Chimie Organique, Université de Poitiers, 40 avenue du Recteur Pineau, 86022 Poitiers Cedex, France
[b] Direction Catalyse et Séparation, Département Catalyse par les Sulfures, IFP, Rond-point de l'échangeur de Solaize, BP 3, 69360 Solaize, France

ARTICLE INFO

Article history:
Received 22 December 2009
Received in revised form 23 March 2010
Accepted 10 April 2010
Available online 24 April 2010

Keywords:
Hydrodesulfurization
Olefin hydrogenation
FCC gasoline
CO
$CoMoS/\gamma\text{-}Al_2O_3$
Edge sites
Density functional theory

ABSTRACT

The selective hydrodesulfurization (HDS) of FCC gasoline is a key catalytic process for reducing sulfur content in gasoline. In addition, 5.75% of the European fuels used for transportation will have to incorporate biofuels, which implies that gasoline hydrotreatment will treat feeds containing various oxygenated compounds including by-products such as CO, CO_2 or H_2O. In the present work, we focus on the effect of CO partial pressure on the transformation of a model FCC gasoline composed of 2-methylthiophene (2MT) and 2,3-dimethylbut-2-ene (23DMB2N) molecules, over a alumina supported CoMoS catalyst. A negative and reversible impact of carbon monoxide on the conversion of 2MT and 23DMB2N is found. Moreover, the hydrodesulfurization (HDS) of 2MT alone is much more inhibited (30%) than hydrogenation (HYD) of 23DMB2N alone (10%). In contrast, when considering the model feed where 23DMB2N and 2MT are mixed together, the loss of HDS and HYD activities is comparable whatever the CO partial pressure. Density functional theory (DFT) calculations of CO adsorption on the S- and M-edge sites of the CoMoS particles show that CO adsorption is strongly favored with respect to olefin and 2MT adsorption on both types of sites, which explains its strong inhibiting effect on HYD and HDS. A rational explanation of the different inhibiting effects of CO observed on model molecules alone and model feed is proposed in correlation with the nature of the active S- and M-edge sites present on the hexagonal CoMoS particles and involved either in HDS or in HYD reactions.

1. Introduction

Residual sulfur of a gasoline feed represents an important polluting agent due to the direct reject of sulfur oxide in the atmosphere and also because of the poisoning of catalytic systems [1,2]. Therefore, a maximal sulfur content for commercial gasoline was fixed at 10 wppm by European Union since 2009 [3], encouraging the research to further improve the efficiency of the alumina supported CoMoS catalysts, well known to be active in hydrodesulfurization reactions. Furthermore, from 2010, in agreement with the decision of the European Commission, 5.75% of the fuels used for the transportation would have to be biofuels [4]. This means that, in the coming years, the gasoline treatment process would be employed to treat many flows from other origins than conventional crude oil. It seems to be especially important to investigate the impact in the refinery of the effluents resulting from the conversion of lignocellulosic biomass feedstocks or from the vegetal or animal oils treatment which will necessarily lead to feeds containing oxygenated compounds (like CO, CO_2 or H_2O) in significant quantity and with many different chemical structures [5–7]. Recent work showed the inhibiting effect of CO in the treatment of diesel cuts [8]. Moreover, the hydrogen stream in the refinery may be a source of CO [9].

Among the different fractions constituting the gasoline pool, fluid catalytic cracking (FCC) gasoline provides up to 90% of sulfur. FCC gasoline is mainly composed by sulfur compounds such as alkylthiophene (15–5000 ppm, depending on the feed geographical origin), C_5 to C_{10} iso-alkenes (20–40 vol%), paraffinic (40–45 vol%) and aromatics (30 vol%) compounds [10–12]. Their high content in olefins (20–40 vol%) is the guaranty of a high octane number [10,13,14] if they are not hydrogenated. Consequently, it is essential to proceed to a deep hydrodesulfurization (HDS) without any hydrogenation (HYD) of the olefinic compounds. Indeed, HDS/HYD selectivity is the key parameter for an efficient gasoline hydrotreating catalyst.

Conventional catalysts for hydrotreating reactions are transition metal sulfide catalysts (TMS) from group VIb such as Mo or W elements promoted by metallic elements from group VIIIb like Ni or Co. For the gasoline hydrodesulfurization, usual catalysts are molybdenum catalysts promoted by cobalt and supported on alumina, with a necessary pre-sulfurization step to activate the cat-

* Corresponding authors. Tel.: +33 549453627; fax: +33 549453897.
E-mail addresses: elodie.devers@ifp.fr (E. Devers), sylvette.brunet@univ-poitiers.fr (S. Brunet).

0926-3373/$ – see front matter © 2010 Elsevier B.V. All rights reserved.
doi:10.1016/j.apcatb.2010.04.005

Table 1
Partial pressures of the different compounds for the sulfidation step and the transformation of the different feeds.

Pressure (bar)	Sulfidation	Olefinic feed	Thiophenic feed	Model FCC gasoline
P_{olefin}	0	1.5	0	1.5
P_{H_2S}	0.1	0.02	0	0
P_{2MT}	0	0	0.03	0.03
$P_{o\text{-}xyl}$	0	0	0	1.9
P_{H_2}	0.9	13.4	13.60	13.11
P_{nC_7}	0	5.07	6.37	3.35
P_{TOT}	1	20	20	20

alyst [15–18]. The atomic scale model of the CoMoS active phase has been refined over the years thanks to the use of various experimental [19–23] and theoretical methods [24,25]. Even if the real active site nature is still widely discussed in the literature, recent Scanning Tunneling Microscopy experiments have shown the existence of a CoMoS mixed phase [26,27] which can be fruitfully confronted with DFT calculations [28,29] in order to describe the CoMoS morphology in HDS conditions. In particular, an hexagonal morphology has been found where two type of edges have been distinguished: S-edge sites fully promoted by Co atoms and M-edge mixed Co-Mo sites exposing Co atoms in the close vicinity of Mo atoms [30,31]. The impact of this morphology on the reactivity of thiophenic compounds [32,33] and olefinic compounds [32] has also been investigated by DFT methods.

Numerous experimental works have attempted to improve the catalytic activity of CoMoS catalysts. Coulier et al. [34] have shown the possibility of using chelating agents during the CoMo catalyst synthesis to improve thiophene HDS activity. It has been shown that CoMo supported phases were better dispersed phases on the support (alumina or silica). An HDS/HYD selectivity gain has been described by Toba et al. [35] with the use of a modified $CoMoP/Al_2O_3$. Some recent studies have demonstrated the importance of the support acido-basicity (use of hydrotalcite or Li/K addition) to improve the HDS/HYD selectivity [36,37]. The study of the transformation of a model feed composed of 2-methylthiophene and 2,3-dimethylbut-2-ene under deep HDS conditions has shown that the modification of the $CoMo/Al_2O_3$ catalyst by potassium decreases both conversions (of alkenes and sulfur compounds). However, the decrease is more significant on the hydrogenation than on the HDS. Consequently, the HDS/HYD selectivity has been improved. Modification of the alumina support by potassium or lanthanum before impregnation of the active phase induces a decrease in the acidity for CoMo catalyst without any modification of the catalyst texture [37]. This type of catalyst has an HDS activity close to the $CoMo/Al_2O_3$, but a lower HYD activity for the treatment of a real gasoline feed (inducing an octane number gain between 4 and 8). Selective catalysts can also be developed by blocking the access to certain type of sites. Hatanaka et al. [38] have shown that the hydrogenation active sites could be preferentially inhibit by coke formation from the olefins of the feed.

As aforementioned, the introduction of oxygenated compounds in the refinery streams, may lead to serious questions about the inhibiting effects of these species. Indeed, it is known that the adsorption of the oxygenated compounds competes with the sulfide ones on catalysts and results to an inhibition on HDS [39]. Moreover, the resulting by-products such as CO, CO_2 or water may also be present in the feeds to be treated and may seriously impact the HDS or Hydrogenation activity of the CoMoS catalysts. A recent kinetic study [9] has shown that CO may indeed exhibit a strong adsorption constant on the catalyst. However, the atomic scale interpretation of the sites inhibition remains still unclear.

In specific analysis conditions such as found in an infra-red characterization chamber, CO used as a probe molecule is well known to strongly interact with the edge sites of MoS_2 and CoMoS catalysts [40,41]. If this is beneficial when CO is used as a probe molecule to describe the structure of the catalysts, high adsorption strengths are suspected to exhibit severe catalytic drawbacks by inducing inhibiting effects for the HDS and HYD reactions.

The aim of this paper is thus to investigate the effect of CO on deep HDS of a model FCC gasoline, represented by 2-methylthiophene (2MT) as model molecule of sulfur compounds and by 2,3-dimethylbut-2-ene (23DMB2N) as model molecule of the olefinic compounds. In order to understand the different phenomena involved, the CO effect is evaluated in two relevant reactions: HDS of 2MT and HYD of 23DMB2N separately and in mixture, in conditions corresponding to those found in a real FCC gasoline. The experimental kinetics results have been interpreted under the light of DFT calculations of the adsorption energies of the different involved reactants and CO and by evaluating the selectivity of adsorption under reactions conditions. A particular attention will be paid to investigate the CO poisoning of the two edge sites of the CoMoS active sites with respect to HDS and HYD reactions.

2. Experimental

2.1. Catalyst and chemicals

The hydrodesulfurization catalyst is a commercial $CoMo/Al_2O_3$ catalyst containing 3 wt% CoO and 10 wt% MoO_3. The catalyst has been crushed, sieved to a 250–315 μm size range and sulfided *in situ* by a H_2S/H_2 flow (10 mol% H_2S) for 10 h at 673 K under atmospheric pressure.

2-Methylthiophene (98% purity) has been purchased from Alfa Aesar, 2,3-dimethylbut-2-ene (98% purity) from Acros Organics, o-xylene (>99% purity) from Fluka and n-heptane (>99% purity) from Carlo Erba. They have been used without any further purification. Carbon monoxide (1% in mixture with H_2) has been purchased from Air Liquide.

2.2. Reaction conditions

Catalytic activity measurements were carried out in a fixed bed reactor at 523 K under a total pressure of 2 MPa with a H_2/feed ratio of 360 L/L as reported in previous works [36]. The feed was injected in the reactor by a HPLC Gilson pump (307 series, pump's head: 5 cm^3). The contact time was calculated by the ratio between the flow of the feed and the volume of the catalyst and was varied from 1 to 60 s. The mass of catalyst varied from 50 to 500 mg, the flow of the feed of 2MT alone and the model feed from 0 to 0.66 mL/min, of the 23DMB2N alone from 0 to 0.2 mL/min and of the CO from 0 to 0.006 mL/h.

Three different types of feeds were studied:

(i) a thiophenic feed containing 0.3 wt% of 2MT (corresponding to 1000 ppm S) in n-heptane,

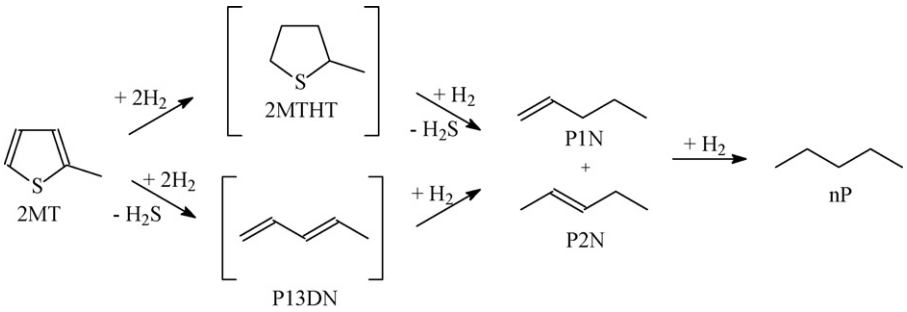

Scheme 1. Reaction pathway of the 2-methylthiophene hydrodesulfurization 2MT: 2-methylthiophene, 2MTHT: 2-methyltetrahydrothiophene, P13DN: pent-1,3-diene, P1N: pent-1-ene, P2N: pent-2-ene, nP: n-pentane

(ii) an olefinic feed containing 20 wt% of 23DMB2N diluted in n-heptane with an additional 1000 ppm S by the introduction of H_2S corresponding to a total 2MT conversion,
(iii) a model FCC gasoline feed containing 0.3 wt% of 2MT, 20 wt% of 23DMB2N, and 30 wt% of o-xylene (representing aromatics) diluted in n-heptane.

The different partial pressures of the reactants are reported in Table 1. o-Xylene and n-heptane were not converted under these experimental conditions.

The impact of CO on 2MT transformation has been evaluated according to the following experimental procedure for the catalytic tests:

(i) transformation of 2MT alone (up to a conversion close to 30%),
(ii) mixture of 2MT and CO with various injections of CO at partial pressures chosen in the range of 0.2–2.4 kPa,
(iii) change of contact time (keeping constant the CO amount) to reach the reference conversions in order to investigate an eventual modification of the products selectivity,
(iv) return to the initial conditions used at step (i) in order to investigate the catalyst deactivation and the modification of the selectivity.

A new experiment was used for each partial pressure of CO on the transformation of 2MT. In contrast, the effect of CO (from 0 to 2.4 kPa) on the conversion of the alkenes has been achieved during the same experiment by verifying that the catalyst can be deactivated over time.

The CO effect has also been studied for the transformation of the model FCC gasoline feed (composed of 2MT, 23DMB2N, and o-xylene in n-heptane) for CO partial pressures between 0 and 1.31 kPa.

2.3. Products analysis

The reaction products have been injected on-line by means of an automatic sampling valve into a Varian gas chromatograph equipped with a PONA capillary column, a flame ionization detector and a cryogenic system [36]. The identification of the products has been performed by GC–MS coupling. According to previous works [36], no significant transformation of o-xylene has been observed, whatever the experimental conditions. Desulfurized products, resulting from the transformation of 2-methylthiophene are designated as HDS products. The selectivity of the reaction will be given by the ratio between HDS and olefin HYD rate constants. HDS and HYD activities were measured after stabilization of HDS and HYD products formation, respectively and under conditions where a linear relationship between conversion and residence time has been obtained (for a yield in HDS products around 30% and the yield in hydrogenation products around of 30%). Regarding the transformation of the 2-methylthiophene, HDS products (mainly pentanes and pentenes) are the main observed products according to the reaction scheme described in the literature [6,12] (Scheme 1). The transformation of the 23DMB2N leads to the formation of isomerization products (mainly 2,3-dimethylbut-1-ene, 23DMB1N) and hydrogenation products (mainly 2,3-dimethylbutane, 23DMB) (Scheme 2). The isomerization of 23DMB2N to 23DMB1N is known to be very fast so that the mixture composed of 23DMB2N and 23DMB1N is considered as the main reactant [36]. The hydrogenation activity has been measured with the formation of 23DMB which was the main hydrogenation product. Skeletal isomers and their hydrogenated products have been obtained with a yield of less than 1%. To obtain the desired conversion (between 0 and 100%), the contact time has been modified by changing the amount of catalyst used (between 75 and 500 mg) or the flow of the feed (0.05–8 mL/min). The catalyst activity (±2%) in hydrodesulfurization corresponding also to the transformation of 2MT is defined as the number of moles of HDS products formed by hour and by gram of catalyst, and the catalyst activity (±2%) in hydrogenation is defined as the number of moles of 23DMB formed by hour and by gram of catalyst. The rate constants were defined by $\log(1/1-\alpha)$ (where α is the conversion of the model molecule) considering that all the catalytic processes studied here are of first order reaction with respect to the reactants.

Carbon monoxide has been analyzed online by a Varian 3800 chromatograph equipped with an automatic sampling valve, two Porapack columns 1 m × 1/8 in. × 2 mm, a methanizer and a flame ionization detector. A backflush procedure has allowed the elimination of H_2S and all other organic compounds (which could poison the methanizer Ni catalyst). Under these experimental conditions and whatever the composition of the model feed, CO has not been converted.

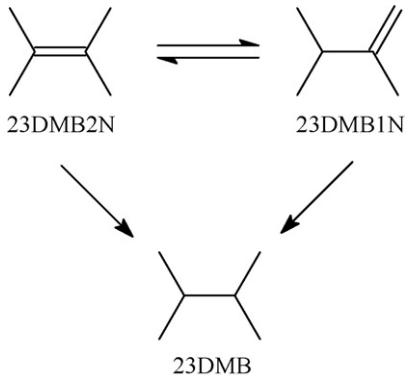

Scheme 2. Reaction pathway of the 2,3-dimethylbut-2-ene hydrogenation 23DMB2N: 2,3-dimethylbut-2-ene, 23DMB1N: 2,3-dimethylbut-1-ene, 23DMB: 2,3-dimethylbutane

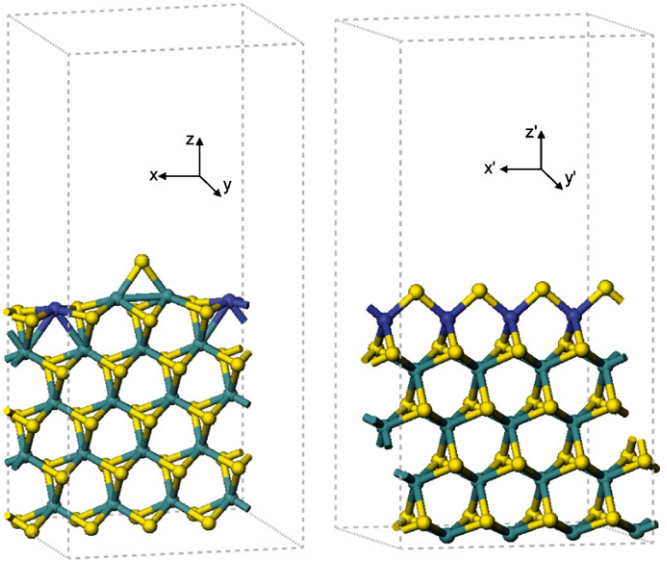

Fig. 1. Examples of unit cells for CoMoS M- (left) and S-edge (right). Most stable configuration of each edges is represented: a promoter content of 50% associated to a sulfur coverage of 12.5% is used for the M-edge, and a fully promoted edge with a sulfur coverage of 37.5% is reported for the S-edge. S atoms are represented in yellow, Mo in green, Co in blue. (For interpretation of the references to colour in this figure legend, the reader is referred to the web version of the article.)

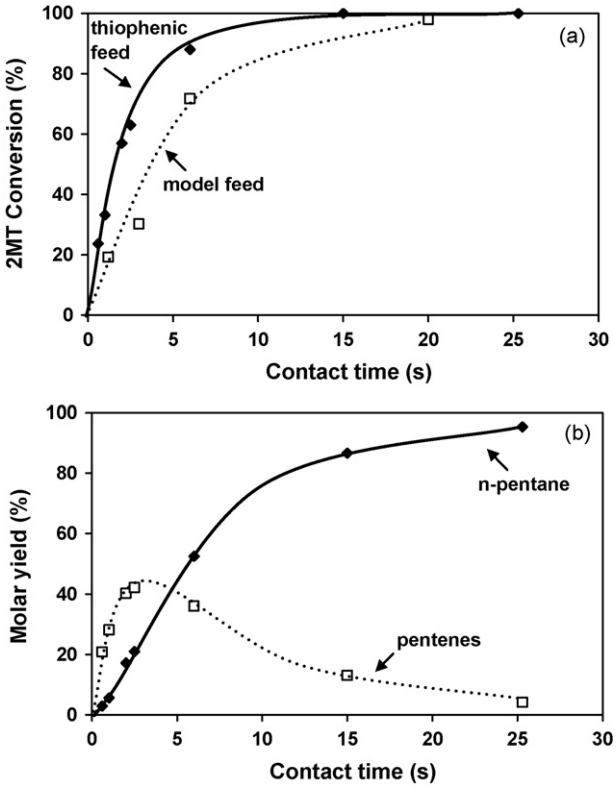

Fig. 2. 2MT transformation (a) conversion versus contact time for the thiophenic (♦, full line) and the model feed (□, dotted line); (b) thiophenic feed products distribution: n-pentane (♦, full line) and pentenes (□, dotted line) (T = 250 °C, P = 2 MPa, H_2/HC = 360 NL/L, CoMo/Al_2O_3).

2.4. DFT calculations

Periodic density functional theory calculations have been performed using the VASP code [42,43]. General gradient approximation with PW91 [44,45] for the exchange correlation functional and the projector augmented-wave (PAW) [46] has been used. The cut-off energy for the plane-wave basis was fixed to 500 eV and the Brillouin zone integration is performed on a (3 × 3 × 1) Monkhorst-Pack k-point mesh. The geometry optimization has been completed when forces become smaller than 0.05 eV Å^{-1}.

Periodic supercells of CoMoS have been modeled according to the previous study of Krebs et al. [32]. The following parameters, 12.29, 12.80 and 27.00 Å, have been used for the supercell, this ensures a vacuum interlayer of 15.00 Å which is sufficient to avoid interactions between the two edges. Hence, in the $z(z')$ direction (Fig. 1), the slab contains four Mo sub-surface layers covered by one mixed Co–Mo metallic row or by a Co row for fully promoted edges. In the $x(x')$ direction, four edges sites have been considered. Various promoter and sulfur contents have been considered, following previous results [33]. The most stable configurations for each edge are reported in Fig. 1.

To study the influence of CO, adsorption competition has been investigated using the same approach as proposed by Krebs et al. [32] for the adsorption of 2MT and 23DMB1N. We compare the CO adsorption energies with those previously found for 2MT and 23DMB1N in [32]. As indicated in the previous paragraph, the transformation of 23DMB2N into 23DMB1N is very fast in order to establish the thermodynamic equilibrium, which justifies the choice of 23DMB1N as a relevant molecule for studying the adsorption competition with CO.

Equations developed in this model have enabled to take into account experimental conditions, in particular the temperature, the $p(H_2S)/p(H_2)$ ratio and the partial pressures of reactants and inhibitor (2MT, 23DMB1N and CO in this study), and then the evolution of the edge energy in presence of an adsorbed molecule has been studied as a function of the $p(H_2S)/p(H_2)$ ratio. Hence the edge energy in presence of adsorbed CO is defined by:

$$\sigma_{edge}(CO) = \sigma_{edge} + \frac{\Delta G_{ads}(CO)}{N} \quad (1)$$

where $\Delta G_{ads}(CO) = \Delta E_{ads}(CO) + RT\ \ln(P_{CO}/P_o) + \Delta G_{trans}(CO) + \Delta G_{rot}(CO) + \Delta G_{vib}(CO)$, and σ_{edge} corresponds to the edge energy without any adsorbed molecule with N the number of edge metallic atoms.

The same definition has been developed for σ_{edge}(23DMB1N) and σ_{edge}(2MT).

To calculate the partition functions of the Gibbs free energy of the adsorbed and gas phase molecules, we have used rigorously the same methodology and approximations as in our previous theoretical work [32]. For sake of clarity, we do not describe them again in the present section and encourage the reader to refer to the methodology section of Ref. [32].

Finally, the adsorption selectivity has been described by the $\Delta\sigma_{edge}$ index, defined as the difference of the edge energies of two adsorbed molecules: $\Delta\sigma_{edge}(A-B) = \sigma_{edge}(A) - \sigma_{edge}(B)$. $\Delta\sigma_{edge}$ is expressed in eV per edge atom and a negative value of $\Delta\sigma_{edge}(A-B)$ indicates a selective adsorption of molecule A to the detriment of molecule B.

3. Results

3.1. Transformation of the various model feeds over CoMo/Al_2O_3

The transformation of the three model feeds, 2MT and alkenes measured separately and the FCC gasoline model feed (2MT and alkenes in mixture) is carried out over CoMo/Al_2O_3 known as a reference for hydrodesulfurization catalyst. The transformation of 2MT and alkenes are thus evaluated alone and in mixture. Fig. 2a

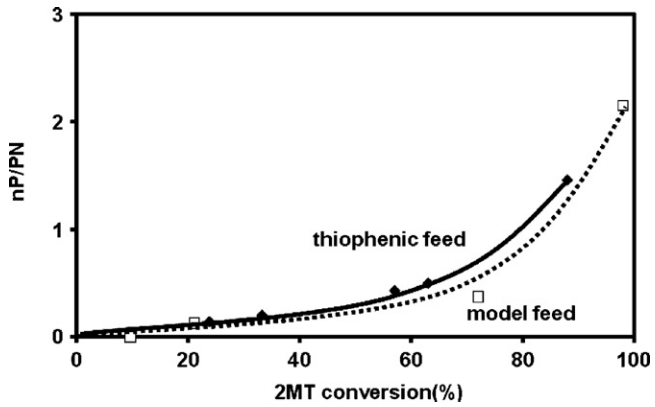

Fig. 3. 2MT transformation. nP/PN ratio (n-pentane (nP) and pentenes (PN)) as function of the conversion of 2MT for the thiophenic (♦, full line) and the model feed (□, dotted line) (T = 250 °C, P = 2 MPa, H_2/HC = 360 NL/L, CoMo/Al_2O_3).

depicts the evolution of the 2MT conversion as a function of the contact time considering the feed composition (2MT alone or in the model feed). The 2MT transformation increases linearly until a conversion close to 70%. The 2MT appears to be less reactive when incorporated in the model feed. For a same contact time (for example, 5 s), the 2MT conversion is significantly lower (around 50%) in the FCC gasoline model feed than in the thiophenic feed (90%). Simultaneously, the complete conversion of 2MT is obtained for higher contact time in the model feed. The two main products of complete desulfurization are C_5 hydrocarbons: n-pentane and pentenes. As shown in Fig. 2b, pentenes (mainly present in the trans-pent-2-ene, cis-pent-1-ene and pent-1-ene forms) are primary products of the reaction which will be then completely hydrogenated in n-pentane at higher conversion (according to Scheme 1). The presence of 23DMB2N and orthoxylene does not modify the distribution between the n-pentane (nP) and pentenes (PN), corresponding to the selectivity between olefinic and hydrogenating C_5. Indeed, the trend is similar whatever the considered feed (thiophenic or model feed) (Fig. 3).

The transformation of 23DMB2N or more exactly the transformation of the alkenes (23DMB2N + 23DMB1N) increases linearly until conversions around 40% (Fig. 4a). The main observed product is the direct hydrogenation product: 2,3-dimethylbutane (23DMB). As seen for the 2MT transformation, the alkenes appeared to be less reactive in the complete model feed: the conversion is lower with the model FCC gasoline than with the olefinic feed for the same contact time.

However, a deactivation phenomenon of the catalyst cannot be excluded during the transformation of olefin alone. Fig. 4b reveals that a loss of 37% of the initial conversion has been observed after 30 h of catalytic treatment (which is not observed during the treatment of the thiophenic feed and the model FCC gasoline feed). This conversion loss is explained by carbon deposition on the catalyst, as indicated by carbon elemental analysis (Table 2) revealing 2.7 wt% of carbon deposition after 30 h of reaction without modification of the sulfur content.

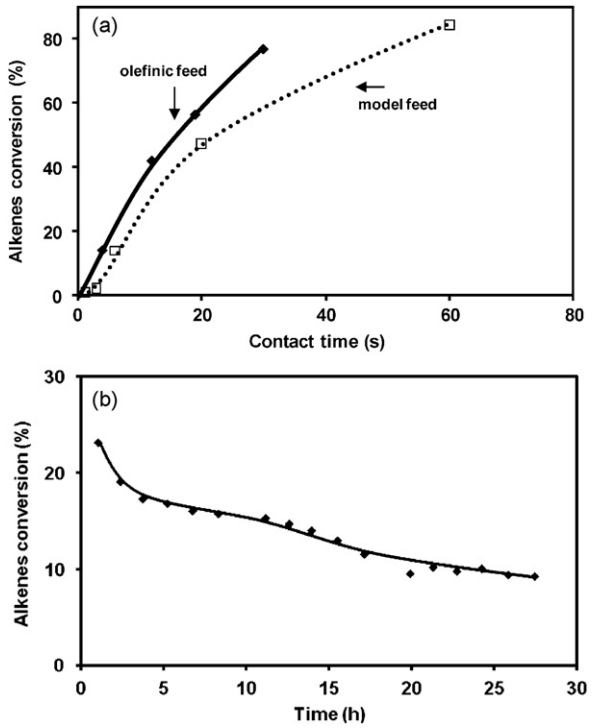

Fig. 4. Alkenes (23DMNB2N + 23DMB1N) conversion (a) olefinic feed (under 1000 ppm H_2S, ♦, full line) and model feed (□, dotted line) as model; (b) olefinic feed as function of time (T = 250 °C, P = 2 MPa, H_2/HC = 360 NL/L, CoMo/Al_2O_3).

Table 2
Alkenes transformation (23DMB2N + 23DMB1N). Catalyst characterization by elemental amount of carbon and sulfur after 30 h of reaction (T = 250 °C, P = 2 MPa, H_2/HC = 360 NL/L, CoMo/Al_2O_3).

	Without CO	With CO
Conversion loss (%)	37	0
C (wt%)	2.7	0.97
S (wt%)	5.0	4.4

These catalytic results can be first explained by a mutual inhibiting effect of the 2MT and the 23DMB2N molecules when using the model FCC gasoline feed (corresponding to a mixture of the 2 substrates). However, it is important to note that only 0.3 wt% of 2MT inhibited a part of the alkenes conversion, while a higher content of 23DMB2N (20 wt%) was necessary to partially inhibit the conversion of the sulfur compound. In order to evaluate the relative impact of the sulfur compound on the alkenes compounds and conversely, the ratio $k_{alone}/k_{mixture}$ between the rate constants of each model molecule alone or in the model feed has been calculated in a large range of conversions (10–80%) (Table 3). The mutual inhibiting impact of both molecules is thus confirmed. Indeed,

Table 3
Transformation of 2MT and alkenes measured separately or in mixture. Change of the reactivity of the model compounds measured by the $k_{alone}/k_{mixture}$ ratio (T = 250 °C, P = 2 MPa, H_2/HC = 360 NL/L, CoMo/Al_2O_3).

	Contact time (s)	1	2	5	10	20
Alone	2MT conversion (%)	34.6	56.1	82.9	100	100
	Alkenes conversion (%)	3.8	7.6	18.3	34.4	60
In mixture	2MT conversion (%)	13.6	26.2	58.6	92	100
	Alkenes conversion (%)	2.7	5.3	12.9	24.8	45.3
$k_{alone}/k_{mixture}$	2MT	2.9	2.7	2	–	–
	Alkenes	1.5	1.5	1.5	1.5	1.5

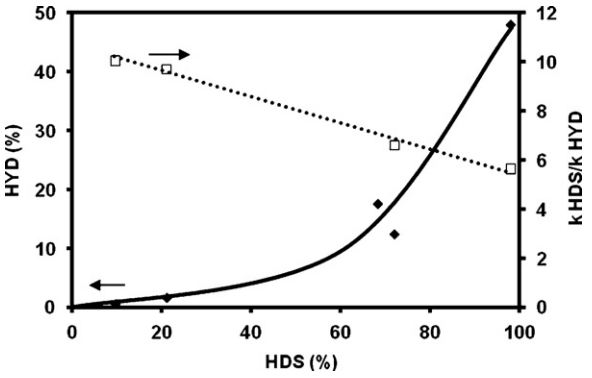

Fig. 5. Transformation of a model FCC gasoline. HYD yield (♦, full line), k_{HDS}/k_{HYD} ratio (□, dotted line) and versus HDS yield (T = 250 °C, P = 2 MPa, H_2/HC = 360 NL/L, $CoMo/Al_2O_3$).

the 2MT conversion seems to be inhibited at low conversion of the alkenes ($k_{alone}/k_{mixture} \sim 3$), however the inhibition decreases with the increase of the alkenes hydrogenation. 23DMB2N transformation appears to be 1.5 more reactive alone than in mixture, no matter the initial conversion, which corresponds to a constant inhibiting effect of the 1000 ppm of S (in the 2MT or H_2S form). These experimental results will be further discussed according to recent ab initio calculations on the adsorption of 2MT and 23DMB1N [32].

The ratio of the rate constants in HDS over HYD which represents the selectivity and the key parameter in gasoline hydrotreatment reactions is reported in Fig. 5. As awaited the selectivity depends on the HDS rate. Indeed, the selectivity decreases linearly with the HDS conversion, which could be explained by the simultaneous increase of the HYD rate when 2MT molecules are converted from the feed which is accompanied by a decrease of their inhibiting effects.

3.2. Influence of CO on 2MT and 23DMB2N alone

The effect of CO on the conversion of 2MT and alkenes alone has been studied for various partial pressures in the range of 0.2–2 kPa. The inhibiting effect of the CO on the transformation of each model molecule (2MT and 23DMB2N) is clearly put in evidence in Fig. 6a. Moreover, the inhibition is observed to be completely reversible since the initial catalytic activities are recovered when the CO flow is stopped. The inhibiting effect is found to be even more significant on 2MT than on olefin conversion. A rapid decrease of the 2MT HDS activity (down to 2.3 mmol h^{-1} g^{-1}) is initially observed until a CO partial pressure of 0.4 kPa. For higher CO partial pressures, the inhibiting effect becomes less pronounced and reaches a plateau. The inhibiting impact of the CO is less important on the olefin HYD and the catalytic activity decreases linearly with the amount of CO added in the feed (Fig. 6a).

After 30 h of catalytic treatment in presence of CO, the catalyst appeared to remain stable for the olefinic feed conversion, contrasting with the previous observation in absence of CO where a deactivation of 37% has been found. For the same duration of the catalytic tests (Table 2), the carbon amount deposited on the $CoMo/Al_2O_3$ catalyst is about 3 times lower than in absence of CO (0.9% compared to 2.7% in absence of CO). Interestingly, this result induces that the coking phenomenon has been inhibited by the presence of CO, preventing catalyst deactivation. These results also showed that the active sites poisoned by the CO might be involved in the coke formation. It is also important to notice that the sulfur amount after the catalytic test is stable and very close to the theoretical sulfidation rate value (considering the catalyst composition) for each experiment.

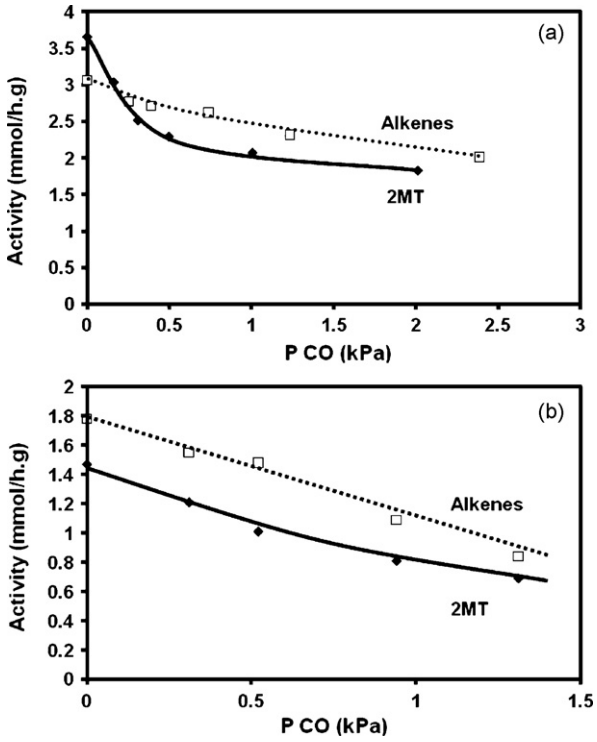

Fig. 6. Impact of the CO partial pressure on the 2MT and the 23DMB2N transformation (a) with 2MT (♦, full line) and alkenes alone (under 1000 ppm H_2S, □, dotted line) alone (b) with 2MT (♦, full line) and 23DMB2N (□, dotted line) in mixture (T = 250 °C, P = 2 MPa, H_2/HC = 360 NL/L, $CoMo/Al_2O_3$).

Table 4
Apparent kinetic orders with respect to CO for the transformation of 2MT and 23DMB2N alone or in the model feed.

		Global order
2MT alone		−0.25
23DMB2N alone		−0.07
Model feed	2MT	−0.12
	23DMB2N	−0.11

From these kinetic results on the transformations of 2MT and 23DMB2N alone, apparent kinetic orders with respect to CO have been evaluated at −0.25 and −0.07 respectively (Table 4), which confirms a more significant inhibiting effect on the 2MT than on the olefinic molecule.

The presence of CO modifies the selectivity measured by the nP/PN ratio in the transformation of 2MT. These results show an amount of pentanes higher in the presence of CO than without. Indeed, for the same conversion of 2MT (30%), the nP/PN ratio increases from 0.19 without CO to 0.27 for a partial pressure of CO of 2.04 kPa (Table 5).

3.3. Influence of CO on model FCC gasoline

The inhibiting effect of CO on the transformation of each molecule in the model FFC gasoline feed is evidenced in Fig. 6b. This inhibition is also completely reversible. No modification of the

Table 5
Change of CO partial pressures on nP/PN (nP: n-pentane, PN: pentenes) ratio for 2MT transformation alone (2MT conversion = 30%) (T = 250 °C, P = 2 MPa, H_2/HC = 360 NL/L, $CoMo/Al_2O_3$).

P_{CO} (kPa)	0	0.16	0.31	0.5	1.02	2.04
nP/PN	0.19	0.23	0.23	0.25	0.28	0.27

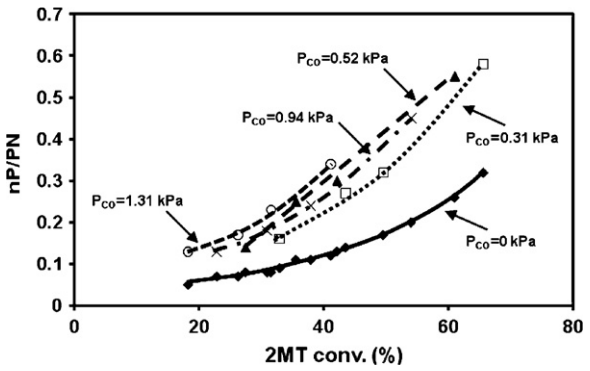

Fig. 7. Impact of the CO partial pressure on the nP/PN ratio (nP: n-pentane and PN: pentenes) as function of the 2MT conversion (T = 250 °C, P = 2 MPa, H_2/HC = 360 NL/L, $CoMo/Al_2O_3$).

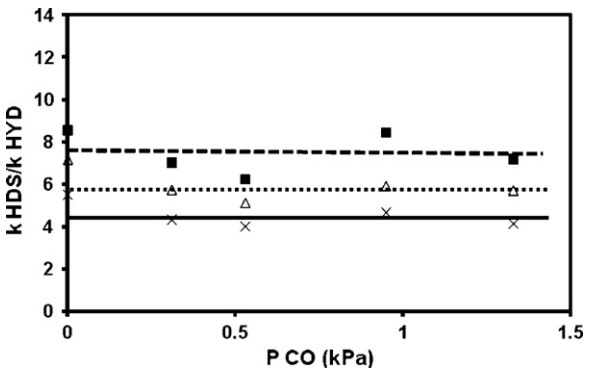

Fig. 8. Transformation of a model FCC gasoline. Effect of different CO partial pressures and initial conversion of 2MT ($C_{0,2MT}$) on the k_{HDS}/k_{HYD} ratio ($C_{0,2MT}$ = 50%: ■, $C_{0,2MT}$ = 59.9%: △, $C_{0,2MT}$ = 79.6%: ×) (T = 250 °C, P = 2 MPa, H_2/HC = 360 NL/L, $CoMo/Al_2O_3$).

products distribution is noticed under these experimental conditions. The catalytic activity for the 2MT transformation decreases almost linearly from 1.47 to 0.69 mmol h^{-1} g^{-1} by the presence of a partial pressure of CO equal to 1.31 kPa, which represents a catalytic activity loss of 53%. For the alkenes transformation, the catalytic activity also decreases linearly from 1.78 to 0.84 mmol h^{-1} g^{-1} for the CO partial pressure, representing a catalytic activity loss of 50%.

The apparent kinetic orders with respect to CO have been evaluated at −0.12 and −0.11 for 2MT HDS and olefin HYD respectively (Table 4), which confirms similar inhibiting effect of the CO regarding the 2MT and the olefinic molecule in the model feed.

The presence of CO is also impacting the products distribution of the 2MT conversion (Fig. 7), as observed for the transformation of the 2MT alone. Whatever the initial conversion of the 2MT (between 38.4% and 79.6%) and whatever the CO partial pressure (between 0.31 and 1.31 kPa), the nP/PN ratio measured is higher than the nP/PN ratio expected (2 times higher for the lower CO partial pressure and 3 times higher for the higher CO partial pressure). The amount of CO seems thus to directly be linked with the increase of the amount of nP obtained (and so to the 2MT transformation selectivity change).

No modification of the k_{HDS}/k_{HYD} selectivity was found due to the presence of CO under these operating conditions (Table 6). For various initial 2MT conversions, the k_{HDS}/k_{HYD} selectivity remains stable whatever the CO partial pressure (Fig. 8). Indeed, for the 2MT conversions of 50%, 59.9% and 79.6%, the k_{HDS}/k_{HYD} selectivity is equal to 6.2, 4.5 and 3.2, respectively. As pointed out previously (Fig. 5), the k_{HDS}/k_{HYD} selectivity decreases principally with the increase of 2MT conversion, no matter the amount of CO added.

Finally, the loss of activity for the transformation of 2MT and 23DMB2N (measured by the ratio between the A activity calculated in presence of P_{CO} = 1.31 kPa and the A_0 activity without CO) induced by adding 1.31 kPa of CO (corresponding to the more significant observed effect) for different nature of the feed is evaluated (Table 7). Different behaviors for the two molecules have been highlighted, depending on the type of feed (molecules alone or model feed). The loss of 2MT HDS activity is similar for the thiophenic feed (A/A_0 = 0.53) and the model FCC gasoline (A/A_0 = 0.47). In contrast, the loss of alkenes HYD activity is close to 25% for the olefinic feed (A/A_0 = 0.75) and significantly increased up to 50% in the model FCC gasoline (A/A_0 = 0.47). Hence, the 23DMB2N conversion is more strongly inhibited with the model feed than with the olefinic feed. Furthermore, the introduction of 1.31 kPa of CO has induced a same relative loss of activity (A/A_0 = 0.47) for the 2 molecules in the model FCC gasoline.

Table 7
Loss of activity A/A_0 (measured by the ratio between the A activity calculated in presence of P_{CO} = 1.31 kPa and the A_0 activity without CO) depending of the feed (2MT and alkenes alone or in mixture).

Feed	2MT alone	Alkenes alone	2MT in mixture	Alkenes in mixture
A/A_0	0.53	0.75	0.47	0.47

3.4. DFT results

CO adsorption is studied on both edges of CoMoS catalyst for different promoter and sulfur contents around the most stable configurations of each edge. To study its inhibition effect towards HDS and HYD, 2MT and 23DMB1N are used to represent theses reactions, in agreement with experiments. For these two molecules previous adsorption results are used [32] and useful structures from this work are recalled. For CO, all possible adsorption positions are studied for all promoter and sulfur contents, nevertheless, for sake of clarity, only the most relevant structures are discussed in this paper.

3.4.1. Adsorption on CoMoS M-edge

Table 8 reports the adsorption energies for the most stable configurations of CO, associated structures for M-edge are represented in Fig. 9, as well as 23DMB1N and 2MT configurations adapted from [32]. According to these results, CO adsorbs preferentially with a linear structure on top of cobalt, thus in the same active site than 23DMB1N and 2MT. Associated adsorption energies are significantly greater compared to the ones already reported for 23DMB1N or 2MT adsorptions. Indeed, for the pairing -Mo-Co-Co-Mo- edge covered by 12.5% of sulfur, CO presents an adsorption energy of −2.05 eV, while adsorption energies of −0.72 and −1.19 eV have been calculated for 23DMB1N and 2MT, respectively. Besides the adsorption energy of CO decreases with the increase of the sul-

Table 6
Change of CO partial pressures on the 2MT and alkenes transformation and the k_{HDS}/k_{HYD} selectivity.

P_{CO} (kPa)		0	0.31	0.52	0.94	1.31
Activity	2MT	1.47	1.21	1.01	0.81	0.69
(mmol h^{-1} g^{-1})	Alkenes	1.78	1.55	1.48	1.09	0.84
k_{HDS}/k_{HYD} selectivity		0.82	0.78	0.68	0.74	0.82

Table 8
Adsorption energies of stable configurations of CO on both edges of CoMoS (see Figs. 9 and 11 for corresponding structures).

Edge	Promoter (%)	S (%)	Adsorption configuration	E_{ads} (eV)
M	50% pair	12.5	3A	−2.05
		25.0	3B	−1.88
	100%	37.5	3C	−1.11
S	100%	37.5	3D	−1.77
		50.0	3E	−0.83
		62.5	3F	−0.87

fur content, hence CO is even more stable for low p(H_2S). These results can be compared to those obtained by Travert et al. [31]. To be as close as possible to our own conditions of promoter and sulfur contents, only their result for the adsorption of CO on the fully promoted M-edge is considered. In that case, they also observe a linear structure with a high adsorption energy of −1.40 eV for a sulfur content of 0%. This is slightly higher than the value of −1.11 eV (configuration 3C) calculated in our conditions, corresponding to a sulfur content of 37.5%. However this evolution is in agreement with the one observed for the partially promoted edge: the adsorption energy decreases as the sulfur content increases.

From this adsorption study, the relative stability of CO compared to 2MT and 23DBM1N under reaction conditions can be evaluated through the edge energies and thus the inhibition effect of CO can be quantified. Experimental parameters are chosen in agreement with conditions used in this present work. Thus the temperature is fixed to 525 K and the following partial pressures are considered: $P_{23DMB1N}$ = 150 kPa and P_{2MT} = 3 kPa. For CO, as performed in experiments, different partial pressures from 0.31 to 2.4 kPa are tested. Besides, calculations are also performed for P_{CO} = 0.0024 kPa, in order to study the inhibiting effect of CO when only a very low partial pressure is considered. Nevertheless we have to note that this pressure cannot be reached in our experimental set-up. For 23DBM1N and 2MT, previous results [32] are adapted with these experimental conditions. Edge energies of adsorbed molecules on the M-edge are represented in Fig. 10, for P_{CO} = 1.31 kPa, and the evolution of the selectivity index of CO versus either 23DMB1N or 2MT is reported in Table 9 for all tested values of P_{CO}.

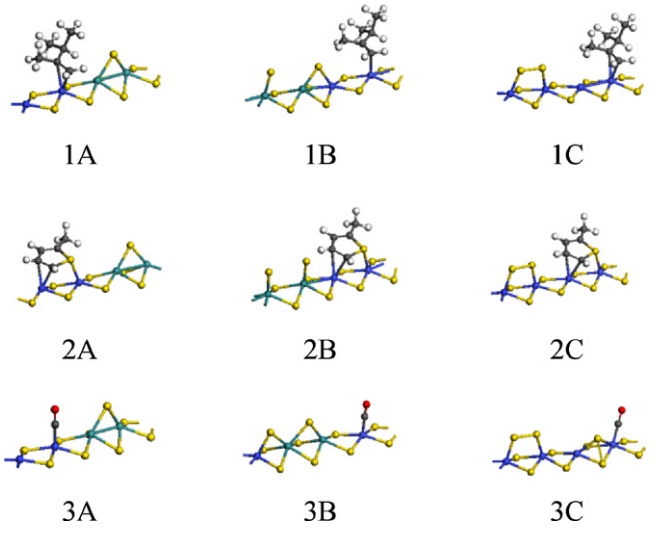

Fig. 9. Adsorption configurations of 23DMB1N (1A, 1B, 1C) adapted from [32], 2MT (2A, 2B, 2C) adapted from [32], and CO (3A, 3B, 3C) on CoMoS M-edge. Structures A and B correspond to the paired partial promotion with 12.5 and 25.0% of sulfur, respectively. Structures C correspond to the fully promoted edge with a S content of 25.0% for 23DMB1N and 2MT and 37.5% for CO.

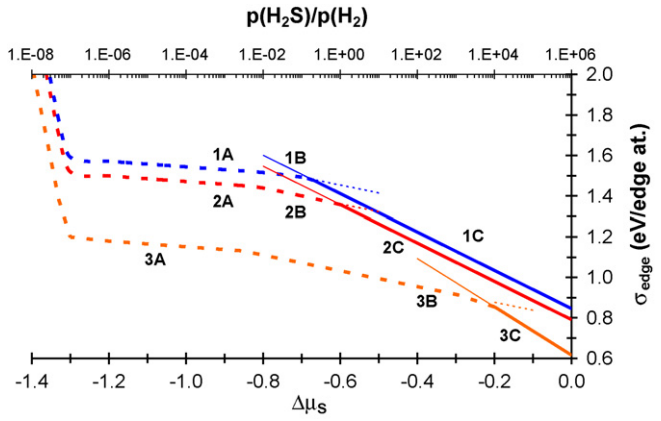

Fig. 10. Evolution of the edge energy (σ_{edge}) as a function of the sulfur chemical potential ($\Delta\mu_s$) for molecules adsorbed on CoMoS M-edge. 23DMB1N, 2MT and CO are represented in blue, red and orange, respectively. Partial pressures and temperature are chosen in agreement with experimental conditions: P(23DBM1N) = 150 kPa, P(2MT) = 3 kPa, P(CO) = 1.31 kPa and the p(H_2S)/p(H_2) axis is determined for T = 525 K. Dashed lines correspond to the partially promoted edge (Co/Mo = 0.5), full lines to the fully promoted one. (For interpretation of the references to colour in this figure legend, the reader is referred to the web version of the article.)

In agreement with the high adsorption energy calculated for CO, the edge energy of CO is always lower than that of 2MT and 23DMB1N. Moreover the inhibition effect of CO is so important, that the change of CO partial pressure between 0.31 and 2.4 kPa has almost no influence on the selectivity index (see Table 9). Even the low value of 0.0024 kPa is not sufficient to induce different behaviors, and in particular a loss of CO inhibition. Thus in the following we will only discuss the case P_{CO} = 1.31 kPa as it is the highest experimental value used for the model FCC feed. Hence, whatever the considered molecule, olefin or thiophene, high selectivity indexes are observed: $\Delta\sigma_{M\text{-}edge}$(CO-23DMB1N) varies from −0.18 to −0.42 eV/edge atom and $\Delta\sigma_{M\text{-}edge}$(CO-2MT) from −0.13 to −0.33 eV/edge atom, depending on the p(H_2S)/p(H_2) ratio. These values can be compared to the low selectivity index calculated between olefin and thiophene molecules: $\Delta\sigma_{M\text{-}edge}$(2MT-23DMB1N) is almost constant between −0.05 and −0.09 eV/edge atom. These results clearly indicate a high inhibition induced by CO.

Regarding the edge configuration, in the case of 2MT or 23DMB1N adsorption, the state of the edge is the same regarding the promoter and sulfur content: the partially promoted edge, with first 12.5% of sulfur, then 25%, is favored up to a sulfur chemical potential around −0.6; −0.7. Then the fully promoted edge with a sulfur content of 25% is observed for higher potential. Moreover, this behavior is identical to the one observed for M-edge without any adsorbed molecules. On the contrary, the presence of CO modifies the preferential configuration of M-edge. In particular, the partially promoted edge becomes stabilized on a larger range of sulfur chemical potential (up to −0.2). Besides the sulfur content for the fully promoted edge is increased to 37.5% instead of 25%, which enhances even more the inhibition effect of CO.

3.4.2. Adsorption on CoMoS S-edge

The same approach is repeated on the S-edge. In line with previous results [32], only the fully promoted edge is considered. Adsorption energies are reported in Table 8 and corresponding structures are represented in Fig. 11. As on the M-edge, CO presents high adsorption energies (−1.77 for the lowest S content) and in particular greater than those calculated in the same conditions for 2MT and 23DBM1N, −1.39 and −0.51 eV, respectively. Nevertheless, for all these molecules, these values remain lower than on

Table 9
Influence of CO partial pressure on the selectivity index between CO and 23DMB1N and between CO and 2MT on the two edges of the CoMoS catalyst. Selectivity index are reported in eV per edge atom. Max and min correspond to the highest and lowest values of the selectivity index as a function of the sulfur chemical potential.

P_{CO} (kPa)	$\Delta\sigma$(CO-23DMB1N)				$\Delta\sigma$(CO-2MT)			
	M-edge		S-edge		M-edge		S-edge	
	Min	Max	Min	Max	Min	Max	Min	Max
0.0024	−0.35	−0.11	−0.37	−0.29	−0.26	−0.05	−0.19	−0.13
0.31	−0.40	−0.16	−0.43	−0.34	−0.31	−0.11	−0.25	−0.18
0.52	−0.41	−0.17	−0.44	−0.35	−0.32	−0.11	−0.25	−0.19
0.94	−0.42	−0.18	−0.44	−0.36	−0.33	−0.12	−0.26	−0.19
1.31	−0.42	−0.18	−0.45	−0.36	−0.33	−0.13	−0.26	−0.20
2.4	−0.43	−0.19	−0.45	−0.37	−0.34	−0.13	−0.27	−0.20

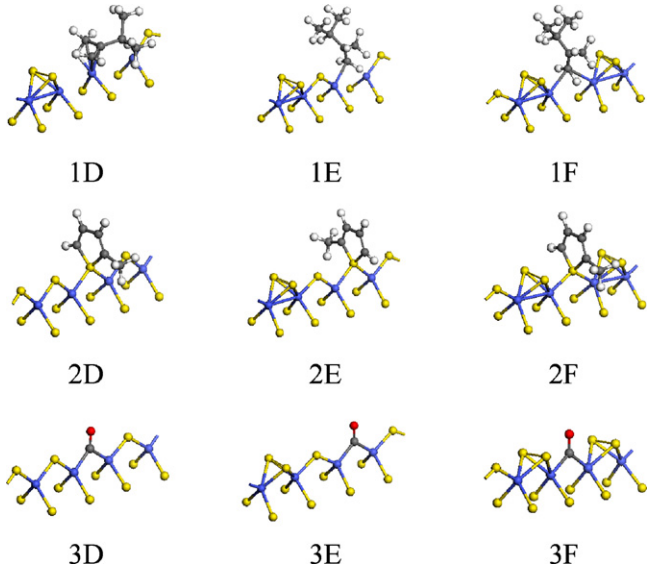

Fig. 11. Adsorption configurations of 23DMB1N (1D, 1E, 1F) adapted from [32], 2MT (2D, 2E, 2F) adapted from [32], and CO (3D, 3E, 3F) on CoMoS S-edge. All structures correspond to the fully promoted S-edge with a S content of 37.5, 50 and 62.5% for the D, E, and F structures, respectively.

the M-edge. Finally, whatever the sulfur content, CO adsorbs on a bridge position in a sulfur vacancy.

The selectivity is now studied through the edge energy. Its evolution in presence of 23DMB1N, 2MT or CO adsorbed on the S-edge of CoMoS is reported in Fig. 12, and the influence of CO partial pressure in Table 9. First of all, as on M-edge, P_{CO} has almost no influence on the evolution of the selectivity index, thus in the following the discussion is done for P_{CO} = 1.31 kPa. Besides, $\Delta\sigma_{S\text{-edge}}$ between 2MT and 23DMB1N is clearly greater than the one observed on M-edge. In fact, it evolves between −0.20 and −0.16 eV per edge atom. This confirms that in our experimental conditions, the selectivity between HDS and HYD is still governed by the S-edge, as it has already been demonstrated by Krebs et al. [32] under different partial pressures of 2MT and 23DMB1N. As on the M-edge, high selectivity indexes are observed when CO is involved. In this way, $\Delta\sigma_{S\text{-edge}}$(CO-2MT) evolves between −0.26 and −0.20 eV/edge atom and $\Delta\sigma_{S\text{-edge}}$(CO-23DMB1N) from −0.45 to −0.36 eV/edge atom. These values indicate a high inhibition effect induced by CO, especially on the olefin. In the forthcoming section, this aspect will be discussed in support of the experimental results.

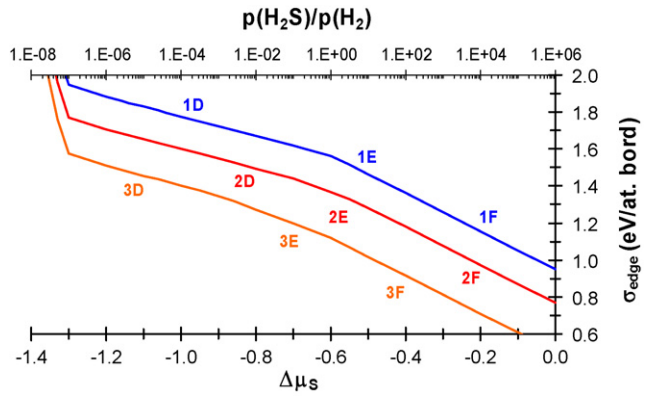

Fig. 12. Evolution of the edge energy (σ_{edge}) as a function of the sulfur chemical potential ($\Delta\mu_s$) for molecules adsorbed on CoMoS S-edge, fully promoted. 23DMB1N, 2MT and CO are represented in blue, red and orange, respectively. Partial pressures and temperature are chosen in agreement with experimental conditions: P(23DBM1N) = 150 kPa bar, P(2MT) = 3 kPa, P(CO) = 1.31 kPa and the p(H_2S)/p(H_2) axis is determined for T = 525 K. (For interpretation of the references to colour in this figure legend, the reader is referred to the web version of the article.)

4. Discussion

The evaluation of the $CoMo/Al_2O_3$ catalyst for the transformation of 3 feeds (thiophenic, olefinic and the complete model feed) allowed us to highlight an important difference of reactivity of these molecules, as they are studied alone or in mixture. Indeed, 2MT and alkenes are both more reactive when they are alone in the feed. This phenomenon demonstrates a mutual inhibition in the model FCC gasoline. However, an amount of 0.3 wt% of 2MT inhibits in part the olefin saturation, while a so much higher amount of olefin (20 wt%) is needed to inhibit in part the conversion of the sulfurorganic compound. The inhibiting effect of 2MT on the olefin is thus higher than the inhibiting effect of the 23DMB2N on the sulfur molecule compound. These results are consistent with the DFT work by Krebs et al. [32], which has highlighted the distinct behaviors of the two edges on the CoMoS mixed phase: S-edge which exhibits the preferential adsorption sites for 2MT and the M-edge, where 2MT and olefin may compete for the adsorption sites. It can be thus understood why a small partial pressure of 2MT strongly inhibits the alkenes hydrogenation. At the same time, it has been shown in [32] that the adsorption selectivity index on the M-edge is not sufficient to counterbalance the kinetic effect in favor of olefin hydrogenation. Hence, even if 2MT is more strongly adsorbed on the M-edge, its adsorption energy is not sufficient to counterbalance the difference in activation energies between HDS and HYD (evaluated at about 50 kJ mol^{-1} [47]). As a result, the olefin reactivity is still possible on the M-edge, as observed experimentally. The inhibition effect thus results from the adsorption competition in favor of 2MT on the S-edge and from the kinetic competition in favor of the olefins on the M-edge.

The inhibiting effect of the CO on the conversion of 2MT and 23DMB2N in independent feeds and in the model FCC gasoline is illustrated by the negative apparent kinetic order of CO on the HDS and HYD reactions. This inhibition is more important on the conversion of 2MT alone than on the conversion of 23DMB2N alone. This trend can also be analyzed considering the DFT calculations on the

CO adsorption on the different types of edge sites. Regarding the DFT adsorption results [32], olefin does not adsorb on S-edge for the considered $p(H_2S)/p(H_2)$ ratio. Hence, the mixed Co-Mo sites located on the M-edge must principally be considered for the HYD reaction and thus the inhibition induced by CO occurs on M-edge. Nevertheless as the HYD activation energy is lower than HDS [47], this reaction still presents a high kinetic rate constant. In contrast, for a $p(H_2S)/p(H_2)$ ratio used in experimental conditions, 2MT has a similar edge energy on both edges. That means that it may adsorb and react on both edges (in absence of CO), however 2MT will also be inhibited by CO both on M-edge and on S-edge. As a consequence, the loss of activity is expected to be greater for 2MT than for 23DMB1N when they are considered alone, because the number of sites active for 2MT HDS (but poisoned by CO) is about twice as high as for 23DMB1N if one assumes an hexagonal shape for the CoMoS nano-particles as proposed by Krebs et al. [32]. Hence, the simultaneous poisoning of mixed M-edge sites and S-edge sites available for HDS may be at the origin of the abrupt loss of HDS activity at low CO partial pressure (with a slope 2 times higher than for olefin HYD as reported in Fig. 6a corresponding to a higher apparent kinetic order for CO).

The second case to be considered is the effect of CO on the model FCC gasoline feed. It appears that the loss of activity is now observed to be similar for 2MT and alkenes when they are considered in the model feed (Table 7 and Fig. 6b). In contrast to the pure thiophenic and olefinic feeds, the slopes of the activity loss in HDS and in HYD are following a very parallel tendency, particularly at low CO partial pressures. This explains why the observed inhibition of active edge sites by CO occurs to the similar extent for olefin and 2MT (with similar kinetic CO kinetic orders). The S-edge sites active for 2MT and the M-edge sites active for olefin HYD [32] are both poisoned by CO. Hence, the simultaneous inhibition of the same amount of HDS S-edge sites and HYD M-edge sites (of the hexagons) will result in the same activity loss for the two reactions. As a consequence, the selectivity (HDS/HYD) remains unchanged either in absence or in presence of CO.

5. Conclusion

By combining kinetic experiments and density functional theory simulation, we have investigated the inhibiting effect of CO on the selective hydrodesulfurization of thiophenic and olefinic molecules. Considering two types of feeds, it has been possible to highlight the effect of CO on the active edge sites of the CoMoS active phase. The feeds containing only either the thiophenic (2MT) or the olefinic compounds has revealed that HDS activity is almost twice as much inhibited than HYD activity at low CO partial pressure. In contrast, when considering the model feed where the olefin and the thiophenic compounds are mixed together, the losses of HDS and HYD activities is almost linear and comparable whatever the CO partial pressure. DFT calculations of CO adsorption on the edge sites of the CoMoS particles have simultaneously shown that CO adsorption energies are strongly favored with respect to olefin and 2MT adsorption energies. Considering the fact that olefin HYD preferentially occurs on the mixed Co-Mo present on the M-edge, while 2MT HDS may occur either on S-edge sites or on the mixed Co-Mo sites present on the M-edge, we have proposed that for pure 2MT reactant, both edge sites are simultaneously inhibited by CO leading to a much stronger loss of HDS activity at low CO partial pressure. In contrast, for the feed where 2MT and olefin are mixed, DFT simulations have shown that the S-edge sites promote HDS of 2MT while the mixed M-edge sites promote olefin HYD. In that case, due to the hexagonal shape of CoMoS particles, a comparable amount of M-edge and S-edge sites are inhibited by CO, which explains the similar loss of HYD and HDS reactivities and thus resulting in similar HDS/HYD selectivities. By combining kinetic experiments with DFT simulation, this work has thus proposed a rational explanation of the inhibiting effect of CO observed on model molecules reactivity in strong correlation with the nature of the active edge sites involved in HDS and HYD reactions.

Acknowledgement

F. Pelardy thanks IFP for a PhD grant.

References

[1] P-O.F. Andersson, M. Pirjamali, S.G. Järas, M. Boutonnet-Kizling, Catal. Today 53 (1999) 565–573.
[2] S. Matsumoto, Catal. Today 90 (2004) 183–190.
[3] Off. J. Eur. Commun. L76/10 (2003).
[4] Off. J. Eur. Commun. L123/42 (2003).
[5] E. Furimsky, Appl. Catal. A 199 (2000) 147–190.
[6] R. Prins, in: G. Ertl, H. Knozinger, J. Weitkamp (Eds.), Handbook of Heterogeneous Catalysis, vol. 4, 1995, pp. 1908–1938.
[7] A.P. Raje, S.-J. Liaw, R. Srinivansan, B.H. Davis, Appl. Catal. A 150 (1997) 297–318.
[8] A. Pinheiro, D. Hudebine, N. Dupassieux, C. Geantet, Energy Fuels 23 (2) (2009) 1007–1014.
[9] P. Ghosh, A.T. Andrews, R.J. Quann, T.R. Halbert, Energy Fuels 23 (2009) 5743–5759.
[10] S. Hatanaka, M. Yamada, O. Sadakane, Ind. Ing. Chem. Res. 36 (1997) 1519–1523.
[11] S. Hatanaka, M. Yamada, O. Sadakane, Ind. Ing. Chem. Res. 36 (1997) 5110–5117.
[12] S. Hatanaka, M. Yamada, O. Sadakane, Ind. Ing. Chem. Res. 37 (1998) 1748–1754.
[13] S. Brunet, D. Mey, G. Pérot, C. Bouchy, F. Diehl, Appl. Catal. A 278 (2005) 143–172.
[14] J.C. Guibet, Technip 1 (1994) (Chapter 5).
[15] C. Brun, T. Saint Pierre, J. Perrot, Hydrocarbon Eng. (1997) 26.
[16] S.T. Oyama, X. Wang, F.G. Requejo, T. Sato, Y. Yoshimura, J. Catal. 209 (2002) 1–5.
[17] J.T. Miller, W.J. Reagan, J.A. Kaduk, J. Kropf, J. Catal. 193 (2000) 123–131.
[18] P. Mazoyer, C. Geantet, F. Diehl, S. Loridant, M. Lacroix, Catal. Today 130 (2008) 75–79.
[19] S. Kasztelan, H. Toulhoat, J. Grimblot, J.P. Bonnelle, Appl. Catal. 13 (1984) 127–159.
[20] H. Topsøe, B.S. Clausen, F.E. Massoth, Hydrotreating Catalysis, Science and Technology, vol. 11, Springer Verlag, 1996.
[21] H. Topsøe, B.S. Clausen, Catal. Rev. Sci. Eng. 26-34 (1984) 395.
[22] R. Prins, V.H.J. De Beer, G.A. Somorjai, Catal. Rev. Sci. Eng. 31 (1989) 1–41.
[23] J.V. Lauritsen, M.V. Bollinger, E. Laegsgaard, K.W. Jacobsen, J.K. Nørskov, B.S. Clausen, H. Topsøe, F. Besenbacher, J. Catal. 221 (2004) 510–522.
[24] P. Raybaud, Appl. Catal. A: Gen. 322 (2007) 76.
[25] J.-F. Paul, S. Cristol, E. Payen, Catal. Today 130 (2008) 139.
[26] J.V. Lauritsen, S. Helveg, E. Laegsgaard, I. Stensgaard, B.S. Clausen, H. Topsøe, F. Besenbacher, J. Catal. 197 (2001) 1–5.
[27] J.V. Lauritsen, J. Kibsgaard, G.H. Olesen, P.G. Moses, B. Hinnemann, S. Helveg, J.K. Nørskov, B.S. Clausen, H. Topsøe, E. Laegsgaard, F. Besenbacher, J. Catal. 249 (2007) 220–233.
[28] P. Raybaud, J. Hafner, G. Kresse, S. Kasztelan, H. Toulhoat, J. Catal. 190 (2000) (2000) 128.
[29] H. Schweiger, P. Raybaud, G. Kresse, H. Toulhoat, J. Catal. 207 (2002) 76–87.
[30] E. Krebs, B. Silvi, P. Raybaud, Catal. Today 130 (2008) 160–169.
[31] A. Travert, C. Dujardin, F. Maugé, E. Veilly, S. Cristol, J.-F. Paul, E. Payen, J. Phys. Chem. B 110 (2006) 1261–1270.
[32] E. Krebs, B. Silvi, A. Daudin, P. Raybaud, J. Catal. 260 (2008) 276–287.
[33] P.G. Moses, B. Hinnemann, H. Topsøe, J.K. Nørskov, J. Catal. 268 (2009) 201–208.
[34] L. Coulier, G. Kishan, J.A.R. Van Veen, J.W. Niemanstsverdriet, J. Vac. Sci. Technol. A19 (2001) 1510–1515.
[35] M. Toba, Y. Miki, T. Matsui, M. Harada, Y. Yoshimura, Appl. Catal. B 70 (2007) 542–547.
[36] D. Mey, S. Brunet, C. Canaff, F. Maugé, C. Bouchy, F. Diehl, J. Catal. 227 (2004) 436–447.
[37] G.H. Tapia, T. Cortez, R. Zarate, J. Herbert, J.L. Cano, Stud. Surf. Sci. Catal. 146 (2003) 685–688.
[38] S. Hatanaka, M. Yamada, O. Sadanake, Am. Chem. Soc., Div. Petrol. Chem. Prep. 42 (1997) 558.
[39] T.R. Viljava, E.R.M. Saari, A.O.I. Krause, Appl. Catal. A 209 (2001) 33–43.
[40] J. Bachelier, M.J. Tilliette, M. Cornac, J.C. Duchet, J.C. Duchet, J.C. Lavalley, D. Cornet, Bull. Soc. Chim. Belg. 93 (8–9) (1984) 743.
[41] F. Maugé, J.C. Lavalley, J. Catal. 137 (1992) 69–76.
[42] G. Kresse, J. Hafner, Phys. Rev. B 47 (1993) 558–561.
[43] G. Kresse, J. Furthmüller, Phys. Rev. B 54 (1996) 11169–11186.
[44] J.P. Perdew, Y. Wang, Phys. Rev. B 45 (1992) 13244–13249.
[45] J.P. Perdew, J.A. Chevary, S.H. Vosko, K.A. Jackson, M.R. Pederson, D.J. Singh, C. Fiolhais, Phys. Rev. B 46 (1992) 6671–6687.
[46] G. Kresse, D. Joubert, Phys. Rev. B 59 (1999) 1758–1775.
[47] A. Daudin, A.F. Lamic, G. Perot, S. Brunet, P. Raybaud, C. Bouchy, Catal. Today 130 (2008) 221–230.